Flow Control Using Magnetic Field in Diverging Microchannel

Aditya Pratap Singh

M. Tech Scholar, Millennium Institute of Technology, Bhopal, India

Abstract: *In the present work, the thermal and hydraulic performance analysis is performed for a diverging microchannel having magneto-hydrodynamic (MHD) pressure-driven flow. Here liquid metal mercury is considered a working fluid where the temperature and flow fields are computed numerically by the finite volume approach with suitable boundary conditions. The present study is carried out using ANSYS Fluent Solver with an add-on MHD module. Working fluid flow is assumed to be steady, laminar, two-dimensional, incompressible, and Newtonian. The hydrodynamic and thermal behavior of working in the micro- channel are studied for different Hartmann number (Ha) of range from $0 \leq Ha \leq 50$, respectively. The introduction of a magnetic field can modify the generation of recirculation zones in diverging sections, as well as the size and strength of the vortices generated. The results show that the dimensions of the recirculation zones decrease with Ha and disappear for moderate Re values. However, for higher Re values, the impact of the magnetic field is negligible. The influence of magnetic field gradient on heat transport is also investigated. The Nusselt number rises as the inclination angle rises. The present design method can also be used for controlling the fluid flow in micro- channels precisely.*

Keywords: Microchannel, Hartmann Number, Nusselt Number, Mercury, and Liquid Flow

1. Introduction

1.1 Microchannel

As per micro- technology, A microchannel is a channel with a hydraulic diameter smaller than one millimeter. Microchannels are employed in the regulation of flow and transfer of heat. In 1981, Stanford Electronics Laboratories researchers Tuckerman and Pease developed the principle of the microchannel for the first time. The compact channels have a large surface area to volume ratio, allowing for rapid heat transfer. The tight channels have a large surface area to volume ratio, allowing for quick heat transfer. Microchannel heat exchangers are tempting in applications where heat exchanger size is limited by space and/or weight or needed effectiveness. Ceramics or metal is used for the fabrication of microchannels. In microchannel Nusselt number varies for fully developed flow. Nusselt number depends on the surface roughness, fluid flow, and Reynolds number. Because of its structural properties, transporting solid materials through a microchannel is difficult. Solid impurities or particles result in the blocking of the microchannel because of the adhesion to the wall and aggregation of molecules, leading to obstruction of the heat transfer rate. The size of the microreactor is between 10 to 1000 microns.

Recently Research endeavors to minimize the size and improving the efficiency of microchips, a little chip with 107 to 10^8 components generates so much heat (100W/cm2) that removing it is a crucial concern for the safety and durability of electronic equipment. Tuckerman and Pease were the first to demonstrate the microchannel cooling technique. Researchers recirculated water in microchannels used on silicon chips, achieving a heat flux of 790W/cm2 without a phase change and a pressure drop of 1.94 bar as compensation. Heat pumps designed for electronics cooling use microchannel heat exchangers in the condenser and evaporator modules. Since the flow in microchannel heat exchangers is frequently laminar, a systemic performance assessment is useful for single-phase heat exchange. Compactness for space-critical applications, sturdy configuration, large volumetric heat transfer, effective flow variation, and modest pressure drops are all benefits of microchannel heat exchangers. Microchannels are the most crucial and focusing points for research topics such as the flow of gases in a microchannel due to significant advantages of this type of channel, such as low density, a high proportion of surface to volume, and their small volume. It has been shown that they have higher heat dissipation capacity than heat removal conventional devices due to exposure to the large surface area to transfer heat for a constant volume of fluid. Fabricators of microchannel nowadays centralize all aluminum materials and brazing construction. Recently microchannel devices inclined towards the HVAC (heating, ventilation, and air conditioning). Numerous researchers have investigated analytical and experimental studies on the thermophysical behavior of microchannels. They've been implemented for the purpose of micro-devices like microreactors, accelerometers for airbag sensors, microreactors, optical switches, inkjet printer heads, computer disc drive heads, micro heat sinks, pressure sensors in blood, projection display chips, microvalves etc. Newton's law of cooling tells that heat transfer rate depends on the surface area and convective heat transfer coefficient at fixed constant temperature difference. Therefore, the final product of hA needs to be increased in order to fulfill the need for substantial heat flux removal, and because the heat transfer coefficient h correlates to the hydraulic diameter, increasing surface area is an option. A small hydraulic diameter and a larger heat transfer area of the channel are recommended for excessive heat transfer, so many narrow channels with a large depth are acceptable. This condition increases the microchannel's pressure drop and hence needs significant pumping power.

1.2 Classification of Microchannels:

Microchannels can be classified based on their geometry (rectangular, circular, trapezoidal, etc.), hydraulic diameter

(sub-millimeter, millimeter, sub-micron), aspect ratio (high or low), flow configuration (single-phase, two-phase, multi-phase), material (metal, polymer, ceramic), and application (electronics cooling, automotive cooling, microreactors, etc.).

1.3 Design Principles

Designing microchannels requires careful consideration of fluid dynamics, heat transfer, and other relevant factors. Key design parameters include channel dimensions, aspect ratio, geometry, surface properties, and flow characteristics. The review discusses the influence of these parameters on fluid flow, heat transfer, and pressure drop within microchannels. It also explores design optimization strategies to improve the performance of microchannel devices.

1.4 Fabrication Techniques

Microchannels can be fabricated using a variety of techniques, including silicon-based microfabrication, soft lithography, micro-electro-mechanical systems (MEMS) technology, and additive manufacturing. Each method has its advantages and limitations in terms of complexity, scalability, material compatibility, and cost. The review provides an overview of these fabrication techniques, highlighting their key features and applications.

2. Literature Survey

Numerous researches have been dealing with the enhancement of the rate of heat transfer in the microchannel. Nowadays, the aim is to save energy with better performance in the development of systems. Microfluidic devices have been recognized in various areas of science and technology because of their vast applications in regions like dynamic cell separators, cell storing, high screening, protein analysis, DNA assay, and high throughput nucleic acid analysis. The main goal in most of these studies is to control the movement working of fluids and separate them, either enhancing the flow or restricting the motion.

Duryodhan et al. (2013) presented a 3D numerical simulation of the working fluid flowing through the diverging microchannel. The working fluid they used was deionized water, where they carried out the impact of diverging angle, length, mass flow rate, and hydraulic diameter on pressure drop. They found that pressure drop increases suddenly at 16° and adverse flow takes place between 12° to 16°. They observed that hydraulic diameter mostly does not depend on the divergence angle, length, and mass flow rate.

Malvandi and Ganji (2014) carried out two-phase modeling of MHD Nanofluid convection in a microtube. They revealed the effects of different properties like nanoparticle slip coefficient, some volume fraction of working fluid, and Hartman numbers on heat transfer. It is drawn to the conclusion that the Nusselt number rises with the increasing Hartmann number.

Song et al. (2018) conducted an analytic solution on the electromagnetic regulation over electrolyte solution flow in the microchannel to know the variation of heat convection with different Hartmann number and Reynolds number. The optimum value Ha number for the better performance of microchannel is 0.05. The entire research is focused on the absence of magnetic field in the microchannel. The aim of this work is to numerically analyze the impact of the magnetic field on hydro-thermal behaviour through a diverging microchannel. The effects of important parameters like the Hartmann number and Reynolds number on the enhancement of heat transfer and fluid properties will be studied in the present work.

Uday Kumar Alugoju and Satish Kumar Dubey (2020) provide a 3D conjugate numerical modeling of a diverging microchannel heat sink utilizing the Volume of Fluid (VOF) model together with the phase change model. The findings show that channels with a small diverging angle (θ) and a low outlet-to-inlet ratio of width (δ) have short nucleation time. Sudden bubble growth and elongated flow as a result of channel restriction were also noted. Heat transfer coefficient values are higher in microchannels with smaller hydraulic diameters and decrease as the diameter increases.

Moolya and Anbalgan (2021) studied the effect of the magnetic field, Prandtl number and Richardson number mixed convection flow in a rectangular body. A SIMPLE algorithm has been used to solve the governing equations with the appropriate boundary conditions using FVM. The authors reported the optimum value of the average Nusselt Number and Sherwood number of 27.35 and 34.79, respectively.

Lei Shi, Wenliang Tao, Nianben Zheng (2022),The focus of this study is on the thermal and fluidic properties of magnetic nanofluids while also taking into account the coupling variables of the magnetic field, thermal exchange, fluidity, and nanoparticle concentration. Entropy generation increases when magnetic field intensity increases due to improved circulation and greater temperature gradient inside the nanofluid.

3. Problem Definition

3.1 Summary of literature review

- The effect of various parameters, such as mass flow rate, velocity, and pressure drop on flow behavior in microchannels are studied.
- Numerical and experimental study of fluid flow with or without magnetic field conducted in the microchannel for various configurations.
- Researchers are trying to implement the Microchannal into the MHD generator.
- Few studies investigated the effect of the magnetic field in different microchannels.

3.2 Research Gap:

- The papers on microchannels present the flow behavior analysis in different geometry like straight, wavy channels, etc.

- Few literatures explored the effect of the magnetic field in the microchannel.
- The use of a magnetic field in diverging microchannels has not been studied.
- The effect of an inclined magnetic field in a microchannel is not reported.

3.3 Objective:

- To study the effect of magnetic field on thermal and flow behavior through a diverging microchannel through numerical simulation.
- To analyze the effects of important parameters such as Hartmann and Reynolds numbers on heat transfer in diverging microchannels.

- To study the effect of an inclined magnetic field in diverging microchannel.

4. Methodology/ Approach

4.1 Geometry

A schematic diagram of the microchannel in three-dimensional considered in this research is shown in Figure 1. The height (H) and length (L) are considered 95 µm and 20 mm, respectively. While smaller width (Wi), larger width (Wo), and hydraulic diameter are 216 µm, 3013 µm, and 177 µm, respectively. The various dimensions of microchannel were taken as per standards of ASHRAE, which was also implied by V. S. Duryodhan (2013).

Table 1: Thermophysical properties of mercury as per Thermal-Fluid Central.

Properties	Cp (J/kg K)	k (W/m K)	ρ (kg/$m3$)	µ (kg/ms)	Pr (105 Pa)	cp,ℓ (kJ/kg-K)
Mercury	139.3	8.54	13529	0.001523	0.0248	0.1353

Table 2: Geometric and Operational Parameters

Geometric and Operational Parameters	Value
Height (H)	95 µm
Length (L)	20mm
Smaller width(Wi)	216 µm
Larger width (Wo)	3013 µm
Hydraulic diameter	177 µm
Temperature at inlet	300 K
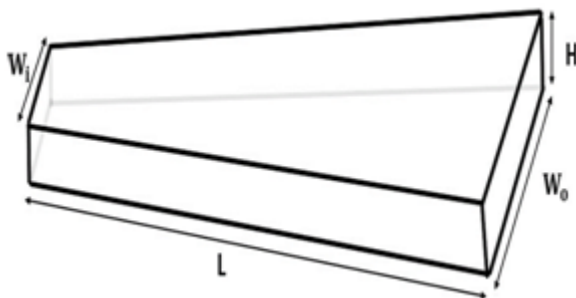
Figure 1: Outline of the diverging microchannel

The inlet temperature of the working fluid is 290 K, whereas the temperature of the lower wall is 360 K, Since various thermophysical properties of mercury are nearly constant in this range. The upper wall and lower walls are adiabatic in this model. The working fluid is assumed to be Newtonian and incompressible. The gravity effect is negligible. These are the assumptions that were used in the present work for the estimation of different dimensionless parameters, and then the governing equations were simplified.

4.2 Governing Equation:
The non-dimensional governing equations for an incompressible Newtonian and electrically conducting fluid flows under the presence of a magnetic field are as follows:

Continuity equation:
$$\nabla \cdot \mathbf{u} = 0 \qquad (1)$$

Where u is the flow velocity.

Navier–Stokes equation:

$$\frac{\partial \mathbf{u}}{\partial t} + (\mathbf{u} \cdot \nabla)\mathbf{u} = -\nabla p + \frac{1}{Ha^2}\Delta^2 \mathbf{u} + N(\mathbf{J} \times \mathbf{B}) \qquad (2)$$

Where p, Ha, N is Stuart number and B are pressure, Hartman number, Stuart number and magnetic field, respectively. The J×B is the Lorentz force.

Current continuity equation:

$$\nabla \cdot \mathbf{J} = 0 \qquad (3)$$

Ohm's law:

$$j = \sigma\,(E + \mathbf{u} \times \mathbf{B}) \qquad (4)$$

Where σ is the solution's conductivity.

Poisson equation for the electrical potential:

$$\nabla^2 \emptyset = \nabla \cdot (\mathbf{u} \times B) \qquad (5)$$

Where $\emptyset$ is electrical potential.

The non-dimensional parameter which appears in above governing equation are Hartmann number (Ha), Reynolds number (Re) and Interaction parameter (N) also known as Stuart number.

4.3 Dimensionless Numbers

Reynolds Number (Re)
The Reynolds number shown above is described by the ratio of inertia force to viscous force.. For the flow to be turbulent Re should be more than 4000 and for flow to be laminar Re should be less than 2000.

$$Re = \frac{Inertia\,force}{Viscous\,force} \sim \frac{\rho u L}{\mu}$$

Hartman Number (Ha):
The Hartmann number can be used as to measure the magnetic field strength. It is defined as the ratio of magneto-electric force to viscous force.

$$Ha = \frac{Electromagnetic\ force}{Viscous\,force} \sim L B o \sqrt{\frac{\sigma}{\mu}}$$

Stuart Number (N):

Relationship between two non-dimensional number i.e., Reynolds number and Hartmann numberis specified by another non-dimensional number known as Stuart number or the Interaction (N). It is the ratio of electromagnetic force to inertia force. The Stuart number is used to estimate the relative importance of a magnetic field on a flow. It is relevant for flows of conducting fluids.

$$N = \frac{Electromagnetic force}{Inertia force} \sim \frac{Ha^2}{Re}$$

Boundary conditions:

At Inlet: A Dirichlet boundary conditions are imposed on all the components of the velocity to control fluxes in thermal and fluid dynamics simulations and imply fixing the derivative of the unknown at specific nodes. Y

i.e., u = 0.32 m/s, v=0 and w = 0.

While for the pressure and electric potential, homogeneous Neumann boundary conditions are specified as:

$$\partial p / (\partial n) = 0, \ (\partial \emptyset) / \partial n = 0$$

At walls: No-slip boundary conditions (u= v= w = 0) are specified at the wall of the channel for the velocity component, and homogeneous Neumann boundary conditions are applied for electric potential.

At outlet: Homogeneous Neumann boundary conditions are stated for each element of velocity and electrical potential, while homogeneous Dirichlet boundary conditions are provided for pressure.

$$\frac{\partial u}{\partial n} = \frac{\partial v}{\partial n} = \frac{\partial w}{\partial n} = 0, \ \frac{\partial \emptyset}{\partial n} = 0$$

4.4 Geometry and Meshing

The geometry for the present simulation cases is created using the three-dimensional tool called SPACECLAIM DISCOVERY is shown in Fig 2.The goal of the tutorial is to construct geometry with the required dimensions and execute CFD analysis based on SI units. This 3D geometry is shown in Figure 2, which is then imported into the meshing operation.
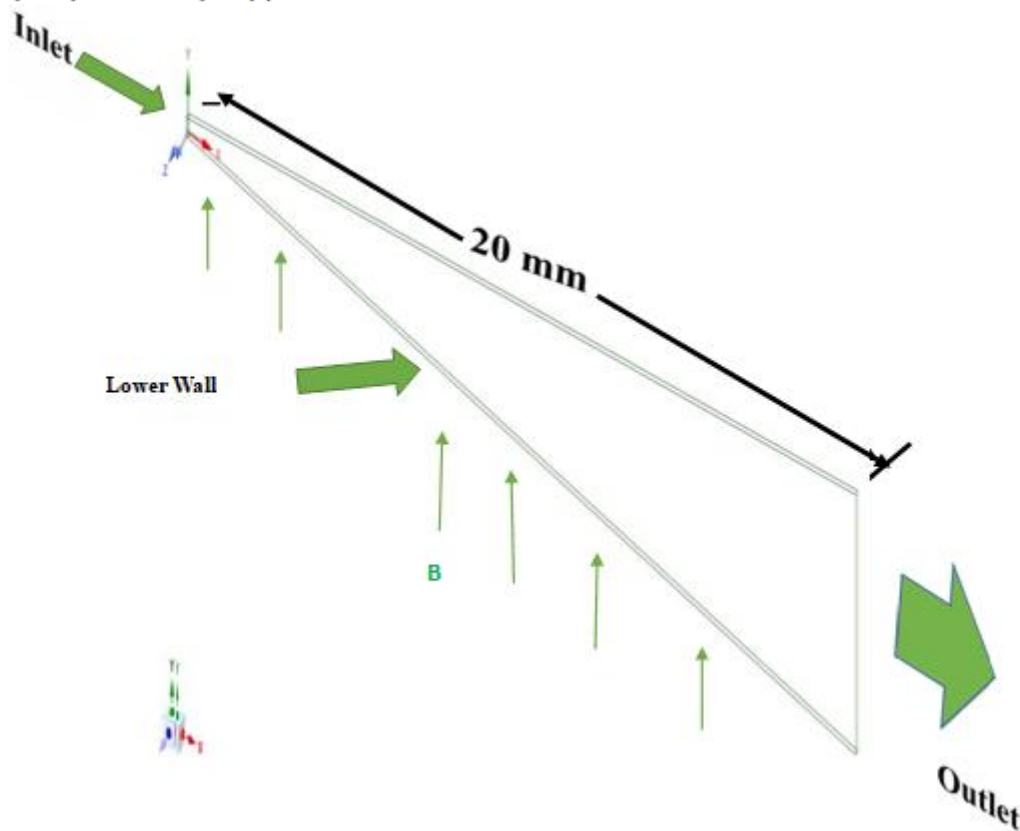
Figure 2: 3D Geometry of diverging micro- channel
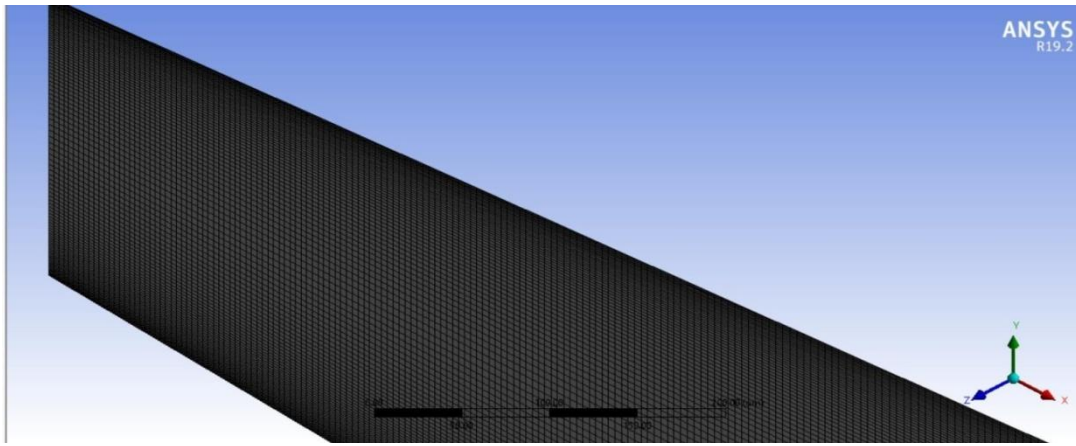
Figure 3: Structured mesh for 2D model
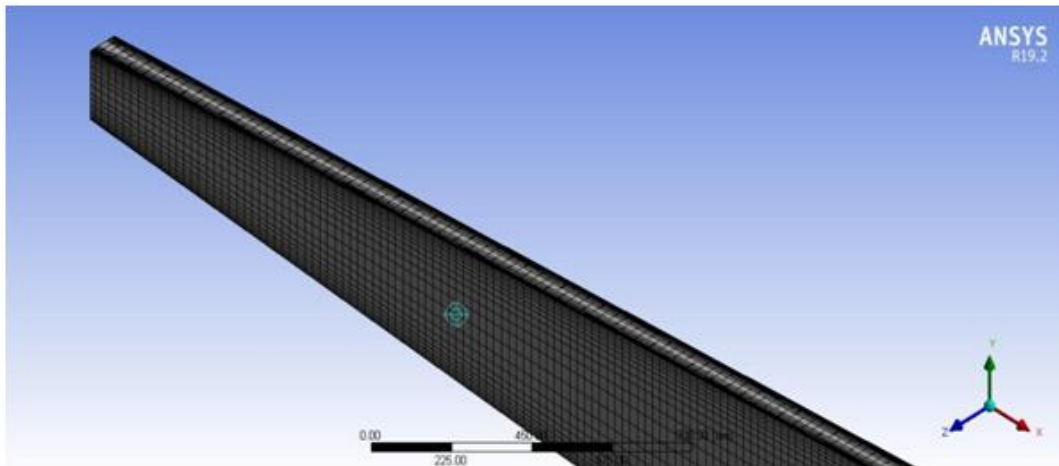
Figure 4: Structured mesh for 3D model

4.5 Grid Independence Test:

To ensure the quality of the developed CFD model, a test for grid dependency on element size is performed. The variation of velocity along the transverse direction (y direction) for three different grid points is plotted in Fig 5. After the grid independence test, it was found that there is a very small variation in the velocity, and the change in flow pattern for different grid sizes is negligible.
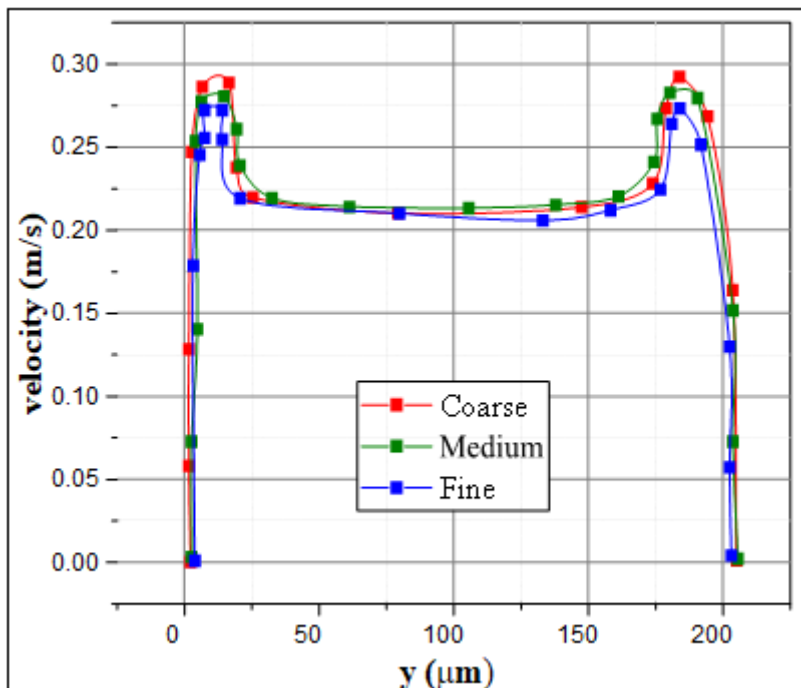
Figure 5: Grid Independence Test

4.6 Validation

The laminar pressure-based solver is used to determine the results numerically in diverging microchannels. The present study is validated with a reference case by Karimipour et al. (2017).
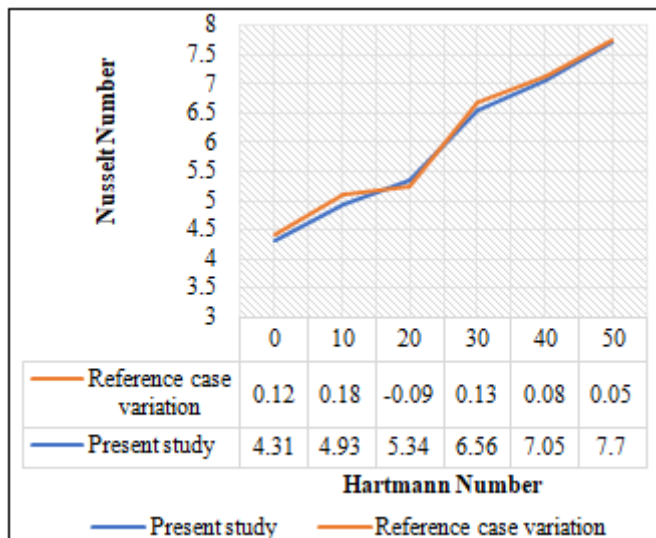
Figure 6: The present study validation with a reference case by Karimipour et al. (2017).

5. Results and Discussions

5.1 Distribution of Velocity

Fig 7.1 depicts the velocity profile in the application of the magnetic field of a range of magnetic fields from Hartman number 10 to 50 and compares it with the fully developed velocity profile. It can be seen from 7 that the velocity near the side layer of the diverging microchannel increases with an increase in the Hartman number increases. Also, the core velocity is lower than the velocity at the side layers of the duct. The effect of electromagnetic force became dominating for a Hartman number greater than 30, and thus M shaped velocity profile is seen for a high Hartman number. For Re = 500 and Ha =10, it is concluded that the inertia force dominated electromagnetic force as the velocity profile is close to the parabolic profile rather than the M shape profile due to magnetic force. Figure 7 also states that the M shape velocity profile seen earlier for a lower Reynolds number compared to a higher Reynolds number for the same Hartmann number.
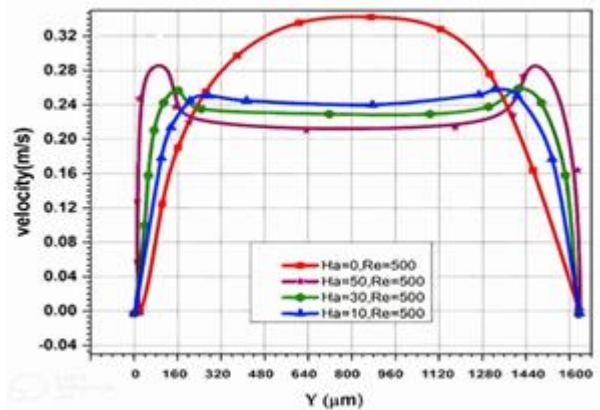
Figure 7.1: Profiles of velocity at different Hartman numbers
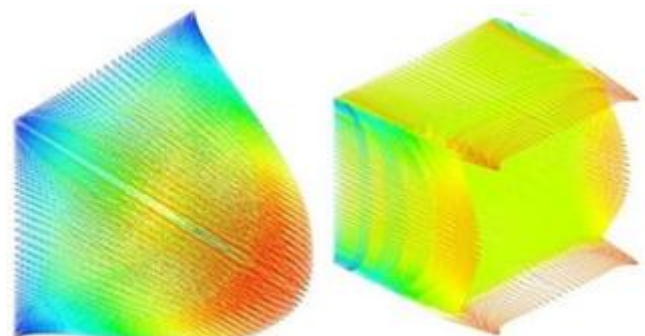
(a) Ha=0 and Re=500 (b) Ha=50 anRe=500
Figure 7.2: Velocity vector

Figure 7.2 shows the velocity vector with and without a magnetic field. The velocity profile at Ha = 0 is fully developed and found to be parabolic, with the maximum velocity at the center core of the diverging microchannel and velocities adjacent to the walls being zero due to no-slip condition. However, on the application of magnetic field at Hartman number 50, the maximum velocity is confined to the region close to walls of diverging microchannel and the core velocity gets reduced. This is mainly electromagnetic force produced to the magnetic field that suppresse the motion of working fluid in microchannel.

5.2 Pressure Distribution:

Fig 8 The variation of pressure along the length of diverging microchannel. In a three-dimensional diverging microchannel, viscous force is dominating, and electromagnetic force, in addition to the viscous, is responsible for steep pressure drop Pressure decreases linearly as the Hartman number increases, and after some distance, it becomes negative because of two dominating forces that are the viscous and electromagnetic forces, resulting in deacceleration for flow. Here the inertia force acting on the microchannel is small in comparison to other forces because of the large length of the microchannel.
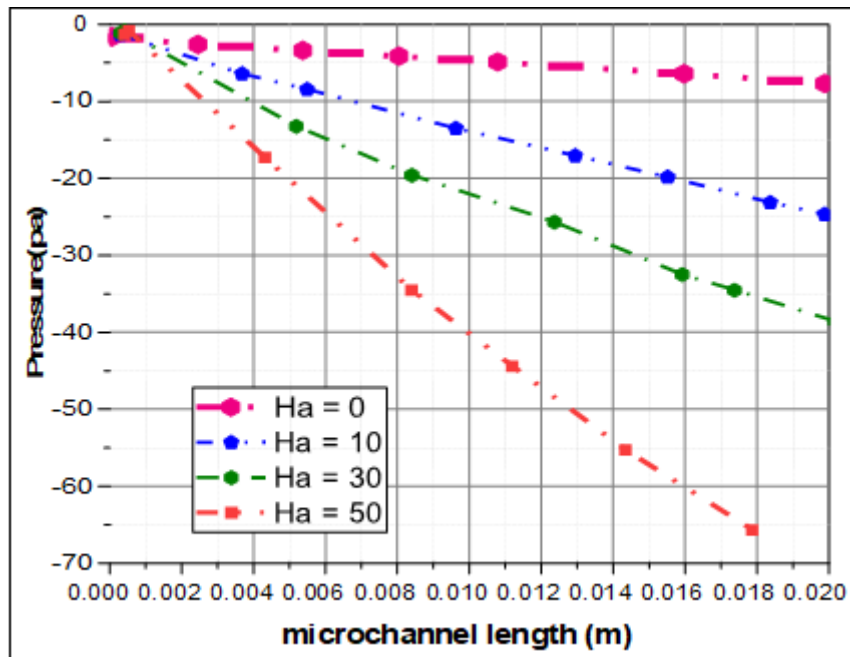
Figure 8: Pressure variation along the length for different Hadrops

Ha = 10, Re = 500
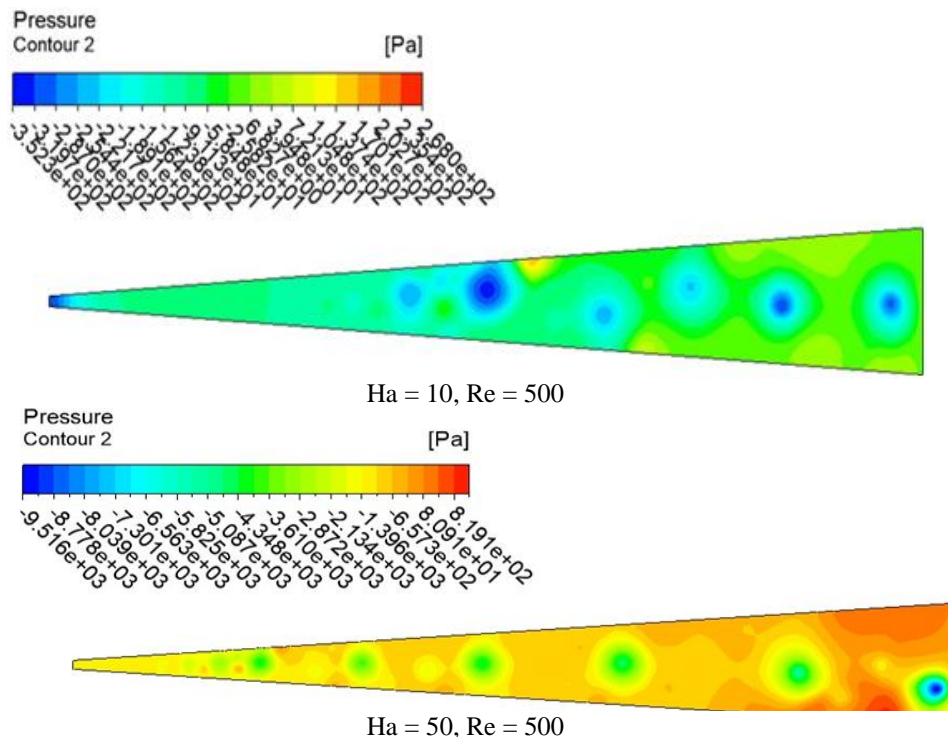
Ha = 50, Re = 500
Figure 9: Pressure contour in 2D

Fig 9 shows the impact of the magnetic field on pressure at different Hartmann number in two- dimensional flow. At the inlet, pressure decreases as the strength of the magnetic field increases. During the motion of the working fluid, eddy formation takes place along the microchannel length. Lorentz force is responsible for the randomness collision of molecules, which results in non-linear variation of pressure.

5.3 Effect of magnetic Field strength on the Nusselt number:

The Nusselt number is a useful tool to study heat convection through the channel. The Nu tells about how much convection heat transfer is taking place. Similarly, Ha indicates the strength of the magnetic field. Nusselt number can be determined at various Hartman number in which mercury is used as the working fluid. The inlet temperature in diverging microchannel is 290 k and the lower wall temperature is 360 k, as various physical properties of mercury remain constant in this range of temperature, and the upper wall is taken adiabatic to remove the heat losses for the study.

Table 3: The Nu variation with microchannel length for different Ha

Microchannel Length	2mm	4mm	6mm	8mm	10mm	12mm	14mm	16mm	18mm
Ha = 0	8.61	5.92	4.91	4.22	3.83	3.21	2.92	2.45	2.14
Ha = 10	11.23	7.73	6.14	4.92	4.12	3.73	3.41	2.82	2.31
Ha = 50	13.13	8.61	6.42	5.23	4.41	3.91	3.62	3.14	2.42
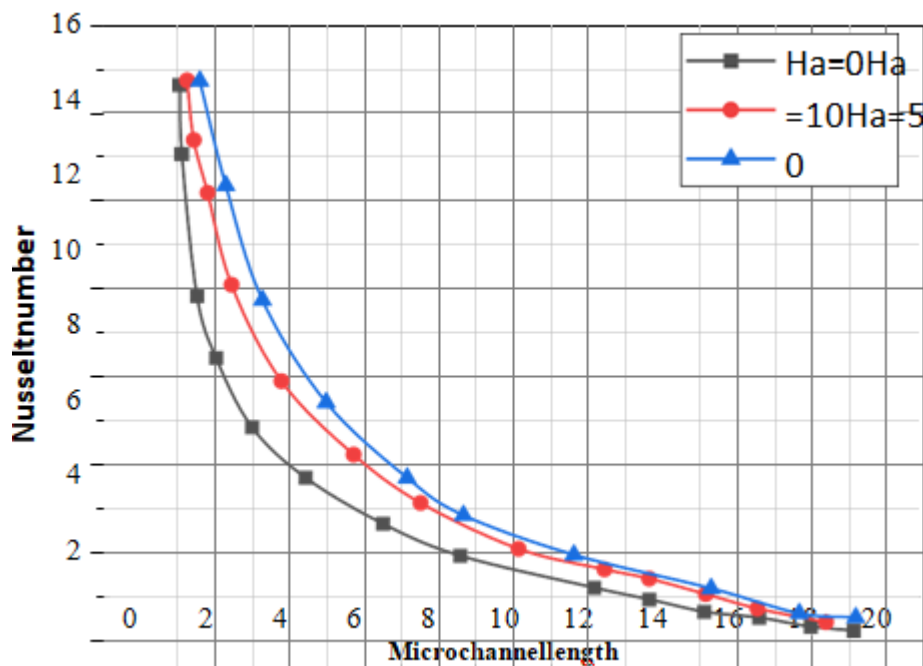
Figure 10: The Nu variation with micro channel length

Fig 10 depicts the local Nusselt number for mercury working fluid along the axial direction of diverging microchannel for different Hartman numbers. Nusselt number is high initially and then decreases along the microchannel length.

Table 4: Variation of Nu with Ha number for different Re

Hartmann Number	0	10	20	30	40
Re = 50	3.42	3.71	4.13	4.42	4.73
Re = 100	4.31	4.92	5.71	6.37	7.12
Re = 200	6.33	6.92	7.54	7.95	8.43
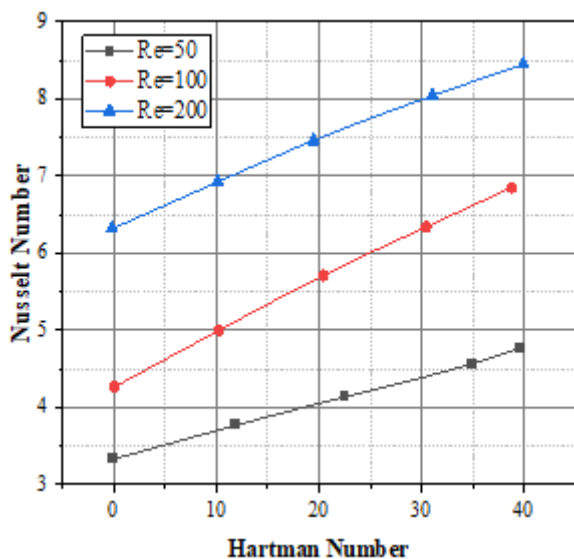
Figure 11: Variation of Nu with Hanumber

Variation of Nusselt number with Hartman number is plotted in Fig 11. It is seen that an increase in the Hartmann number increases the Nusselt number. This is mainly due to the formation of the vortices at higher Hartman. The formation of vortices induces the motion, which causes the increase in Nusselt number, leading to an increase in convective heat transfer.

5.4 Effect of incline magnetic field on convection heat transfer in diverging microchannel

The inclination angle is defined as an angle between the longitudinal axis of the microchannel and the applied magnetic field, as shown in Fig 12. A good method to change the Nu number significantly is to change the direction of magnetic field. The electromagnetic force is applied to the microchannel by changing the direction of the magnetic field.
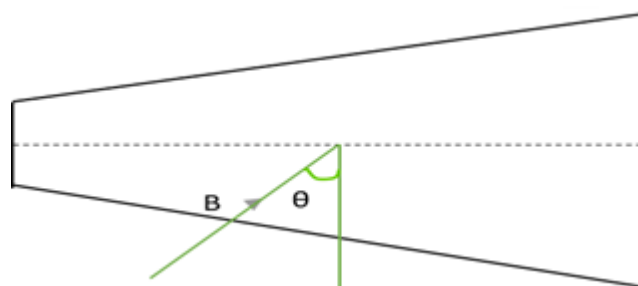
Figure 12: Two-dimensional cross section having inclined magnetic field

Table 5: Distribution of Nu with inclined magnetic field for different Ha

Inclination Angle	50	60	70	80	90
Ha = 10	2.13	2.62	4.72	6.41	7.13
Ha = 30	3.72	4.21	7.33	8.21	9.62
Ha = 50	5.33	6.21	9.12	10.22	10.43
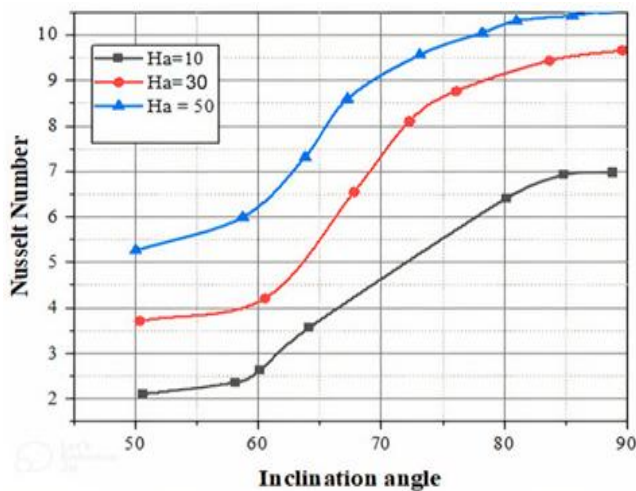
Figure 13: Distribution of Nu with the inclined magnetic field

Fig 13 depicts the variation of the Nusselt number at various inclination angles. It is seen that the Nu number increases as the inclination angle increases. At 90º, the Nu number approaches its maximum. It demonstrates that increasing the Ha number improves convection mobility.

6. Conclusion

The effect of magnetic field on flow behavior and heat transfer in 3D and 2D diverging microchannel is numerically investigated. To enhance the condition, the present study has the analytic simulation in diverging microchannel with the effect of a magnetic field. It is seen that the Nusselt number rises as the Hartman number rises. Also, the electromagnetic force is dominant over inertia and viscous force, and this causes to change the velocity profile alter from parabola to M shaped. It indicates that the velocity at the mid-section of the diverging microchannel is lower than the peak velocity of the side layers. An enhancement in the strength of the magnetic field enhances the formation of vortices as electromagnetic force dominates over viscous and inertia forces. It is also found that the inclination of the magnetic field has a noticeable effect on fluid motion. Further, An increase in inclination angle increases the Nusselt at various fixed parameters. Numerical simulation results show that liquid-metal electrical conductivity has a major influence on the liquid-metal flow. The present design method can also be used for controlling the fluid flow in microchannels precisely.

7. Future Scope

- The optimum parameters can be identified with C.F.D. for the different types of microchannels.
- Exergy analysis can be formed to know and improve the efficiency of the microchannel.
- The system performance of micro-channel can be improved by changing the construction material.
- The effectiveness of the system can also be enhanced by changing the type of working fluid.

References

[1] Stieglitz, R., Barleon, L., Bühler, L., and Molokov, S., 1996, "Magnetohydrodynamic Flow in a Right-Angle Bend in a Strong Magnetic Field," J. Fluid Mech., 326, pp. 91–123.

[2] Leboucher, L., 1999, "Monotone Scheme and Boundary Conditions for Finite Volume Simulation of Magnetohydrodynamic Internal Flows at High Hartmann Number," J. Comput. Phys., 150(1), pp. 181–198.

[3] Smolentsev, S., Morley, N., and Abdou, M., 2005, "Code Development for Analysis of MHD Pressure Drop Reduction in a Liquid Metal Blanket Using Insulation Technique Based on a Fully Developed Flow Model," Fusion Eng. Des., 73(1), pp. 83– 93.

[4] Andreev, O., Kolesnikov, Y., and Thess, A., 2006, "Experimental Study of Liquid Metal Channel Flow under the Influence of a Nonuniform Magnetic Field," Phys. Fluids, 18(6), pp. 1–12.

[5] Yan, Y., Yang, S., and Kim, C. N., 2016, "Three-Dimensional Features of MHD Flows Turning in a Right-Angle Duct," J. Mech. Sci. Technol., 30 (12), pp. 5459–5471.

[6] Raisi, A., Ghasemi, B., & Aminossadati, S. M., 2011, "A numerical study on the forced convection of laminar nanofluid in a microchannel with both slip and no-slip conditions." Numerical Heat Transfer, Part A: Applications59, pp. 114-129.

[7] Selimli, S., Recebli, Z. and Arcaklioglu, E., 2015, "MHD numerical analyses of hydrodynamically developing laminar liquid lithium duct flow." International Journal of Hydrogen Energy, 40, pp.15358-15364.

[8] Molokov, S., and Btthler, L., 1994, "Liquid Metal Flow in a U-Bend in a Strong UniformMagnetic Field," J. Fluid Mech., 267, pp. 325–352.

[9] Vantieghem, S., Albets-Chico, X., and Knaepen, B., 2009, "The Velocity Profile of Laminar MHD Flows in Circular Conducting Pipes," Theor. Comput. Fluid Dyn., 23(6),pp. 525–533.

[10] Smolentsev, S., Moreau, R., Bühler, L., and Mistrangelo, C., 2010, "MHD Thermofluid Issues of Liquid-Metal Blankets: Phenomena and Advances," Fusion Eng. Des., 85(7–9),pp. 1196–1205.

[11] Malvandi, A. and Ganji, D. D., 2014, "Magnetohydrodynamic mixed convective flow of Al2O3–water nanofluid inside a vertical microtube." Journal of Magnetism and Magnetic Materials 369, pp.132-141.

[12] Gajbhiye, N. L., and Eswaran, V., 2015, "Numerical Simulation of MHD Flow and Heat Transfer in a Rectangular and Smoothly Constricted Enclosure," Int. J. Heat Mass Transf.,83, pp. 441–449.

[13] He, Q., Feng, J., and Chen, H., 2016, "Numerical Analysis and Optimization of 3D Magnetohydrodynamic Flows in Rectangular U-Bend," Fusion Eng. Des., 109–111, pp.1313–1317.

[14] Manca, O., Nardini, S., Khanafer, K., and Vafai, K., 2003, "Effect of Heated Wall Position on Mixed Convection in a Channel with an Open Cavity," Numer. Heat Transf.Part A Appl., 43(3), pp. 259–282.

[15] Swain, P. K., Satyamurthy, P., Bhattacharyay, R., Patel, A., Shishko, A., Platacis, E., Ziks,A., Ivanov, S., and Despande, A. V., 2013, "3D MHD Lead-Lithium Liquid Metal Flow Analysis and Experiments in a Test-Section of Multiple Rectangular Bends at Moderate to High Hartmann Numbers," Fusion Eng. Des., 88(11), pp. 2848–2859.

[16] Lu Yang, Jing Tan, Kai Wang, Guangsheng Luo, 2013, "Mass transfer characteristics of flow in microchannels" he State Key Laboratory of Chemical Engineering, Department of Chemical Engineering, Tsinghua University, Beijing 100084, China.

[17] Malvandi, A. and Ganji, D. D,. "Magnetohydrodynamic mixed convective flow of Al2O3–water nanofluid inside a vertical microtube." Journal of Magnetism and Magnetic Materials 369(2014), PP: 132-141.

[18] Sahu P. K., Golia A. and Sen A. K., 2012, "Analytical, numerical and experimental investigations of mixing fluids in microchannel." Microsyst Technol 18, pp. 823–832.

[19] Holden MA, Kumar S, Castellana E, Beskok A, Cremer PS (2003) Generating fixed concentration arrays in a microfluidic device. Sensor Actuat B Chem 92:199–207.

[20] Duryodhan VS, Singh SG and Agrawal A., 2013, " Liquid flow through a diverging microchannel." Microfluid Nanofluid 14, pp.53–67.

[21] Mehta SK and Pati S., 2020, " Thermo-hydraulic and entropy generation analysis for magnetohydrodynamic pressure driven flow of nanofluid through an asymmetric wavy channel." International Journal of Numerical Methods for Heat & Fluid Flow, pp. 0961-5539.

[22] Mayeli, P., Hesami, H., Besharati-Foumani, H. and Niajalili, M., 2018, "Al2O3–water nanofluid heat transfer and entropy generation in a ribbed channel with a wavy wall in the presence of magnetic field", Numerical Heat Transfer, Part A: Applications, Taylor and Francis, Vol. 73 No. 9, pp. 604-623.

[23] Mayeli, P., Hesami, H., Besharati-Foumani, H. and Niajalili, M., 2018, "Al2O3–water nanofluid heat transfer and entropy generation in a ribbed channel with a wavy wall in the presence of magnetic field", Numerical Heat Transfer, Part A: Applications, Taylor and Francis, Vol. 73 No. 9, pp. 604-623.

[24] Azad, A. K., Rahman, M. M., and Oztop, H. F., 2014, "Effects of Joule Heating on Magnetic Field inside a Channel along with a Cavity," Procedia Eng., 90, pp. 389– 396.

[25] Moolya S and Anbalgan S., 2021, "Optimization of the effect of Prandtl number, inclination angle, magnetic field, and Richardson number on double-diffusive mixed convection flow in a rectangular domain." International Communications in Heat and Mass Transfer 126, 105358

[26] Tiwari, N. and Moharana, M.K., 2019, "Comparative study of conjugate heat transfer in a singlephase flow in wavy and raccoon microchannels", International Journal of Numerical Methods for Heat and Fluid Flow, Vol. 30 No. 7, pp. 3791-3825.

[27] Del Giudice, C. Nonino, and S. Savino., 2007, "Effects of viscous dissipation and temperature dependent viscosity in thermally and simultaneously developing laminar flows in microchannels," Int. J. Heat Fluid Flow, vol. 28, no. 1, pp. 15–27

[28] F. Hedayati and G. Domairry,2016, "Nanoparticle migration effects on fully developed forced convection of TiO 2–water nanofluid in a parallel plate microchannel," Particuology, vol. 24, pp. 96–10

[29] Karimipour A., D'Orazio A. and Mostafa S. S., 2017, " The effects of different nano particles of Al2O3 and Ag on the MHD nano fluid flow and heat transfer in a microchannel including slip velocity and temperature jump" , Physica E, vol 86, pp.146-15.

Author Profile

Aditya Pratap Singh

adityaprop448@gmail.com
DOB: 13/03/1997
B.E.in Mechanical Engineering
M.Tech in Thermal Engineering